ACTA RADIOLÓGICA PORTUGUESA
May-August 2026 | Vol 38 nº 2 | e45530 https://doi.org/10.25748/arp.45530

**Review Article / Artigo Revisão**

# Beyond Bone Metastasis: Unveiling Non-Metastatic Mimics

## *Para Além das Metástases Ósseas: Desvendando os seus Mimetizadores*

**Maria Inês F. Ribeiro[1], Miguel Oliveira e Castro[2]**

[1]Medical Doctor (Radiology resident); Radiology Department, Instituto Português de Oncologia (IPO) de Lisboa Francisco Gentil, Lisboa, Portugal
[2]Medical Doctor (Radiologist); Radiology Department, ULS Algarve - Hospital de Portimão, Portimão, Portugal

**Address**

Maria Inês Fernandes Ribeiro
Departamento de Radiologia
Instituto Português de Oncologia (IPO) de Lisboa Francisco Gentil
Rua Professor Lima Basto
1099-023 Lisboa, Portugal
e-mail: mariainesfr@gmail.com

**Received:** 17/02/2026
**Accepted**: 13/03/2026
**Published**: 02/04/2026

**Abstract**

Bone metastases are common in the oncological setting, and their diagnosis is usually evident. Nonetheless, differentiating malignant from benign lesions can present significant challenges, as various benign musculoskeletal conditions may mimic metastatic processes. Consequently, specialised intervention by a radiologist is fundamental to establish a correct diagnosis and guide therapeutic strategy. This article reviews four benign entities initially interpreted as possible metastases, highlighting that definitive diagnosis relies on an integrated approach, combining imaging features, clinical and laboratory data, and, when ambiguity persists, biopsy and histological confirmation.

**Keywords**

Bone metastasis; Bisphosphonates; Osteoporotic fractures; Brown tumour; Calcific tendinopathy.

**Resumo**

As metástases ósseas representam uma entidade frequente em contexto oncológico, cujo diagnóstico é, habitualmente, evidente. Contudo, a diferenciação entre lesões malignas e benignas coloca por vezes desafios significativos, já que diversas patologias musculoesqueléticas benignas podem sugerir clinicamente processos metastáticos. Torna-se por isso fundamental a intervenção especializada do Radiologista para esclarecer o diagnóstico e orientar a conduta terapêutica. Este artigo revê quatro entidades benignas inicialmente interpretadas como metástases, enfatizando que o diagnóstico definitivo exige uma abordagem integrada, combinando achados imagiológicos, dados clínicos e laboratoriais e, em casos de persistente ambiguidade, a realização de biópsia.

**Palavras-chave**

Metástase óssea; Bisfosfonatos; Fraturas Oosteoporóticas; Tumor castanho; Tendinopatia calcificante.

## Introduction

Bone metastases are a frequent finding in the oncological setting, and their diagnosis is usually straightforward. Nevertheless, several benign disorders are often misinterpreted as metastatic disease, particularly when the full clinical context is not considered and multidisciplinary expert opinions are not sought. Such cases can be diagnostic challenges, occasionally necessitating biopsy for confirmation. In this article, we review four musculoskeletal lesions initially misinterpreted as bone metastases in the clinical setting: bisphosphonate-related atypical femoral fractures, vertebral osteoporotic compression fractures, brown tumours of hyperparathyroidism, and gluteus maximus calcific tendinopathy. Our focus is primarily on the imaging features that enable a definitive and accurate diagnosis, highlighting the crucial role of specialised radiological assessment in the diagnostic pathway.

## Bisphosphonate-Related Atypical Femoral Fracture

A 58-year-old woman under follow-up for breast carcinoma was receiving bisphosphonate therapy for a remote history of bone metastasis. She presented to the emergency department following trauma to the left thigh, reporting severe pain and functional limitation. The radiograph showed a complete subtrochanteric fracture of the femoral diaphysis (Fig. 1). Retrospective evaluation of a scout image from a follow-up thorax, abdomen, and pelvis CT acquired 10 months earlier revealed lateral cortical thickening of the left femur in a subtrochanteric location (Fig. 2), which had gone unnoticed

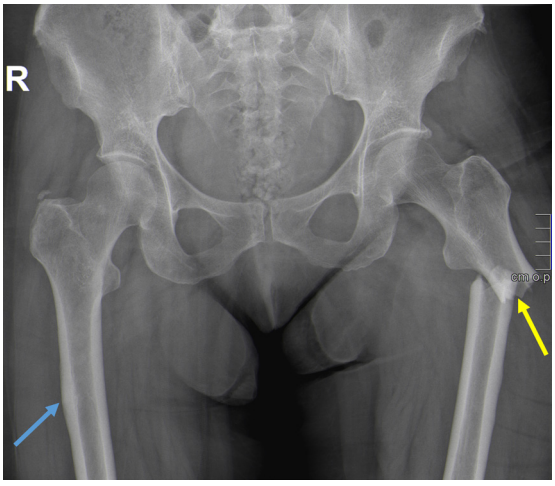


**Figure 1** – Pelvic radiograph demonstrates a subtrochanteric fracture of the left femoral diaphysis (yellow arrow), typical of a bisphosphonate-related atypical fracture. Lateral cortical thickening of the right femur in a subtrochanteric location is also present (blue arrow).

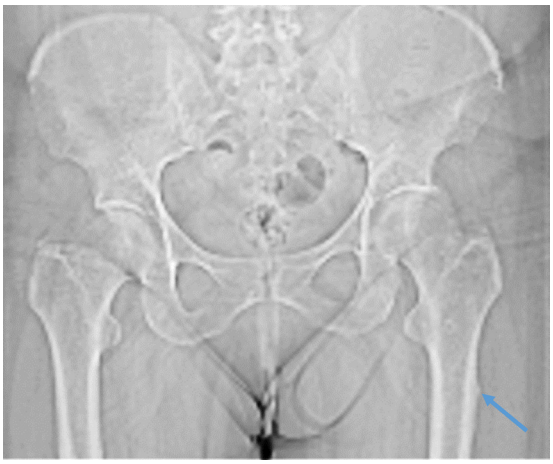

**Figure 2** – Scout image of a follow-up abdominopelvic CT, obtained 10 months before the fracture depicted in fig. 1, demonstrates a faint lateral cortical thickening of the left femur in a subtrochanteric location (blue arrow).

at the time. These findings are typical of a bisphosphonate-related atypical femoral fracture. Nevertheless, the fracture was clinically assumed to be pathological, secondary to bone metastasis from breast carcinoma. No radiologist was consulted. The patient was treated with intramedullary nailing, and bisphosphonate therapy was continued.

Four years later, a similar fracture occurred in the right femur (Fig. 3), which was again clinically interpreted as a pathological fracture. Retrospective evaluation of scout image from a previous CT scan acquired 15 months earlier showed evidence of an atypical femoral fracture developing at the lateral cortex of the right femoral diaphysis (Fig. 4). This fracture was also treated with intramedullary nailing. On this occasion, however, a biopsy was performed, and showed no evidence of neoplastic tissue.

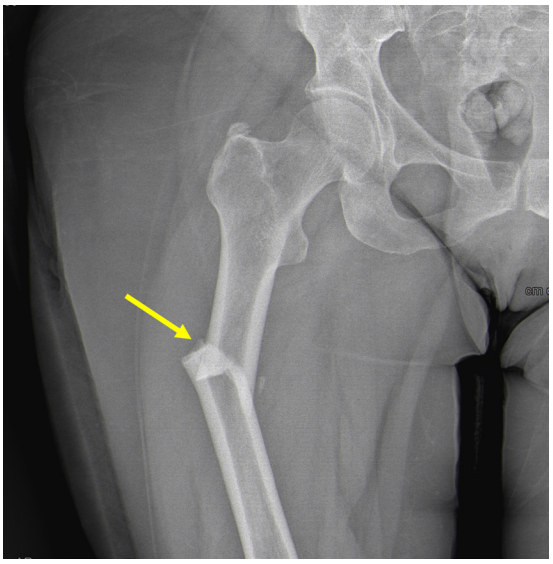

**Figure 3** – Hip radiograph demonstrates a subtrochanteric fracture (yellow arrow) of the right femoral diaphysis, occurring one year after the scout image shown in Fig. 2.

A musculoskeletal radiologist was consulted, who made the diagnosis of bisphosphonate-related atypical femoral fractures. The patient showed no evidence of metastatic lesions elsewhere in the skeleton, and treatment was modified, including cessation of bisphosphonate therapy. Bisphosphonates are a class of drugs commonly used

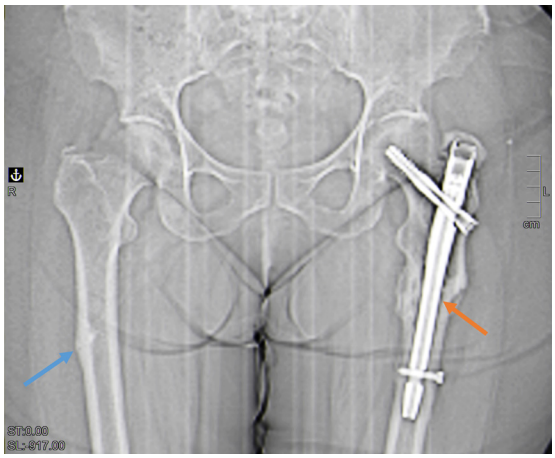

**Figure 4** – Scout image from another follow-up abdominopelvic CT, acquired 15 months before the second fracture shown in fig. 3, shows an intramedullary nail (orange arrow) from previous fixation of a left femoral fracture, with fracture callus in the subtrochanteric region. In the right femur, lateral cortical thickening is observed (blue arrow), representing a prodromal radiological sign of a bisphosphonate-related atypical femoral fracture.

in the treatment of osteoporosis in the elderly.[1,2] They are also effective bone-targeted therapies for patients with bone metastases, particularly those arising from breast cancer, prostate cancer, and multiple myeloma.[3,4] Their mechanism of action consists of inhibiting osteoclast-mediated bone resorption, thereby increasing bone mineral density.[5] However, long-term use is associated with atypical femoral fractures.[2,6] This complication is thought to result from suppressed bone turnover, accumulation of microdamage, and increased bone mineralisation. Consequently, bone becomes brittle, may fail under normal physiological stress, and may demonstrate delayed healing.[7,8]

Patients typically describe dull, aching thigh or groin pain weeks to months before fracture occurrence.[9,10] These fractures usually originate in the lateral cortex of the upper third of the femur in a subtrochanteric location,[1,11] distinguishing them from osteoporotic fractures, which most commonly involve the femoral neck or intertrochanteric region.[1]

Radiological features of atypical femoral fractures include initial lateral cortical thickening (beaking), followed by a transverse or short-oblique fracture that may initially be incomplete and subsequently progress to a complete, non-comminuted fracture[12] at the aforementioned site. Approximately one in three to four patients presents with bilateral involvement,[1] underscoring the importance of imaging the contralateral femur, even in the absence of symptoms.

Management includes discontinuation of bisphosphonate therapy and surgical intervention for both complete and incomplete fractures.[13]

## Vertebral Compression Fractures

A 77-year-old man with a history of prostate adenocarcinoma, treated with a combination of radiotherapy and androgen deprivation therapy three years earlier, presented with sudden-onset back pain. CT images revealed generalised decreased bone density suggestive of osteopenia/osteoporosis (Fig. 5), with endplate compressions involving T12, L2, and L3 (Fig. 6A), which were symmetrical on coronal reconstruction (Fig. 6B). There was no extension to the posterior elements,

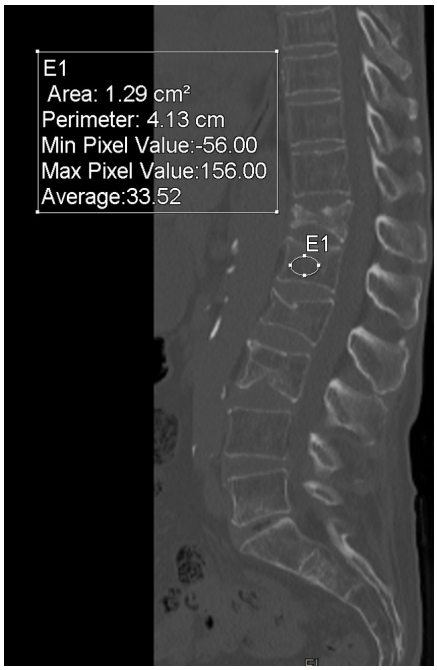


**Figure 5** – Coronal non-enhanced CT reconstruction in bone window reveals a vertebral attenuation of 33,5 HU in L1, consistent with osteoporosis.

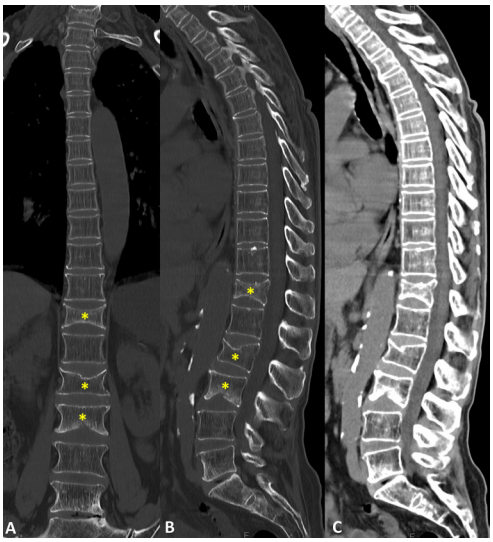


**Figure 6** – Coronal (A) and sagittal (B) non-enhanced CT reconstructions in bone window, acquired four days after symptom onset, demonstrate endplate compression fractures (yellow asterisks) involving T12, L2, and L3, which are symmetrical on the coronal plane. Sagittal non-enhanced CT reconstruction in soft-tissue window (C) shows no associated soft-tissue mass.

including the pedicles, and no associated soft-tissue component (Fig. 6C). Although the CT report favoured benignity, these fractures were initially interpreted clinically as bone metastases.

A biopsy showed no evidence of neoplasia, although the sample was deemed insufficient for definitive assessment. The patient underwent MRI (Fig. 7), which demonstrated a well-defined T1 hypointense signal localised to the T12 fracture site, as well as to the upper endplate of L1, with no involvement of the posterior elements or associated soft-tissue mass. Collectively, these findings supported a diagnosis of osteoporotic rather than pathological fractures. Following consultation with a musculoskeletal radiologist, the vertebral collapses were defined as benign.

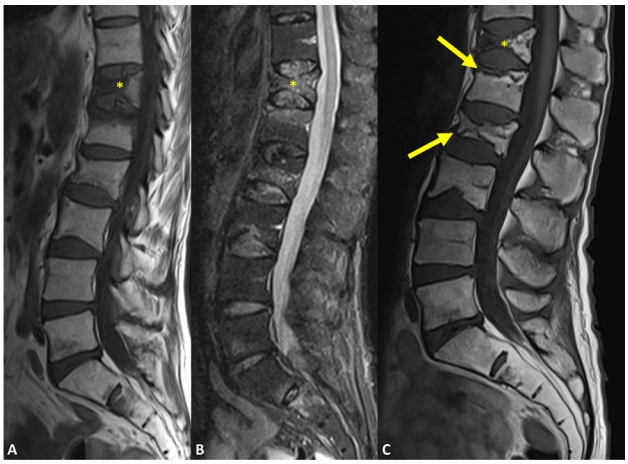


**Figure 7** – Sagittal T1-weighted (A) MRI images acquired one month after symptom onset, demonstrate further collapse of the T12 body (yellow asterisk), with well-defined T1 low signal and bone marrow oedema localised to T12 body and the adjacent L1 endplate, without involvement of the posterior elements or an associated soft-tissue mass. These findings are consistent with progression of T12 collapse and impending L1 fracture. Sagittal STIR (B) demonstrates faint bone marrow oedema in the L2, L3, and L5 vertebral bodies. Sagittal T1-weighted MRI image (C) acquired one year after symptom onset shows increased collapse of the T12 (yellow asterisk), L2, and L3 vertebral bodies and development of fracture lines in L2 and the upper endplate of L1 (yellow arrows).

Indeed, acute osteoporotic vertebral compression fractures can mimic pathological fractures caused by metastatic disease on MRI, making differentiation challenging, particularly in older adults and in patients with known primary tumours.[14] Certain imaging features favour a neoplastic cause, including diffuse vertebral body involvement with low T1 signal and complete fatty marrow replacement, pedicle or posterior element involvement, a convex or bulging posterior vertebral border, an epidural or paraspinal soft-tissue mass, and additional focal lesions in other bones.[14,15]

Conversely, osteoporotic fractures typically show a linear low-signal-intensity band on T1- and T2-weighted images parallel to the endplate (fracture line or trabecular compaction) (Fig. 7C), marrow signal sparing (islands of preserved high T1 fat) within the collapsed body, and posterior bony retropulsion of a cortical fragment, rather than a soft-tissue mass.[16] In addition, chemical-shift imaging may be useful, as an in-phase and out-of-phase signal drop greater than 20% is suggestive of benignity.[17]

T2-weighted imaging is generally not helpful in distinguishing benign from malignant fractures.[14]

Given the clinical importance of accurate differentiation, MRI features alone are often insufficient. If diagnostic uncertainty persists, follow-up MRI after six to eight weeks or biopsy is recommended.[14] Osteoporotic fractures typically show partial or complete resolution of marrow signal abnormalities on follow-up imaging, whereas metastatic lesions usually remain unchanged or demonstrate progression.

## Brown Tumours of Hyperparathyroidism

A 25-year-old male patient with an unremarkable medical history presented to the emergency department with pain following a low-energy injury to the right arm. A shoulder radiograph revealed a central lytic lesion in the proximal humerus with pathological fracture (Fig. 8). A CT scan of the shoulder was subsequently obtained to further characterise the lesion and additionally demonstrated a lytic lesion in a rib (Fig. 9), raising suspicion of bone metastasis.

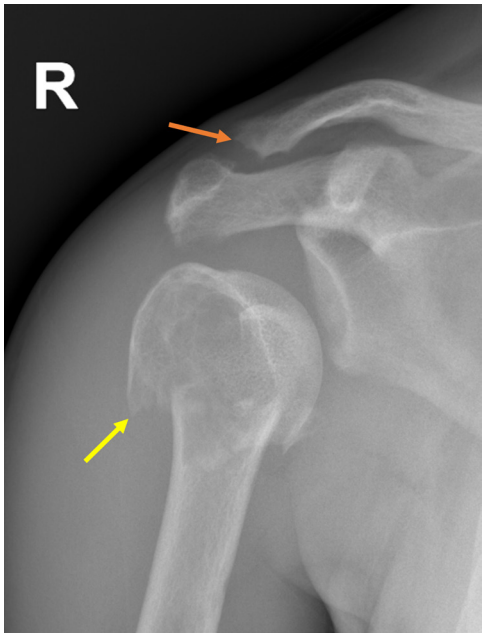


**Figure 8** – Shoulder radiograph demonstrates a central lytic lesion in the proximal humerus with a pathological fracture (yellow arrow). There is a narrow zone of transition, with no periosteal reaction or evident soft-tissue mass, features favouring a benign, non-aggressive process. Bone resorption of the acromioclavicular joint surfaces is also present (orange arrow).

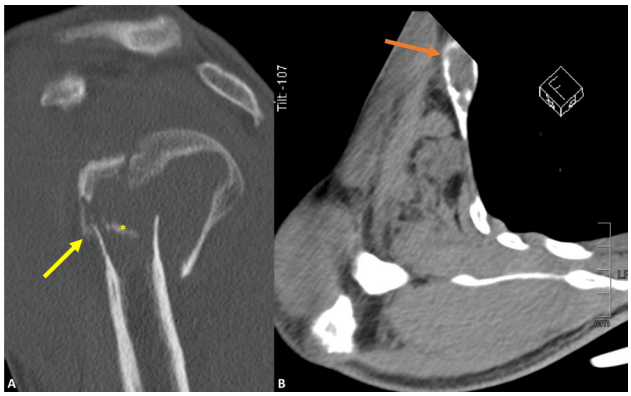


**Figure 9** – Non-enhanced CT of the right shoulder. Sagittal CT reconstruction in bone window (A) and axial CT image in soft-tissue window (B) demonstrate a fractured central lytic lesion in the proximal humerus, with a narrow zone of transition and no periosteal reaction (yellow arrow), favouring a benign process, as well as a lytic lesion in a rib (orange arrow). A fallen fragment is present within the lesion (yellow asterisk), a sign often observed in, but not specific to, simple bone cysts.

Consequently, a CT scan of the thorax, abdomen and pelvis was performed to search for a primary tumour. This revealed multiple lytic lesions in the ribs and pelvis, as well as a cystic mass in the parathyroid gland (Fig. 10). Cytology suggested a parathyroid tumour, and the parathyroid hormone (PTH) level measured in the fine-needle aspiration washout fluid was elevated. Accordingly, the lytic lesions in the axial skeleton and shoulder were interpreted as brown tumours of hyperparathyroidism (HPT), rather than metastatic disease.

Additional imaging findings consistent with HPT were present, including acro-osteolysis of the phalangeal tufts and subperiosteal resorption along the radial aspects of the middle phalanges of the hands, as well as a brown tumour on a toe in hand and foot radiographs (Fig. 11). Bone resorption at the acromioclavicular joint surfaces was also evident on the shoulder radiograph (Fig. 8).

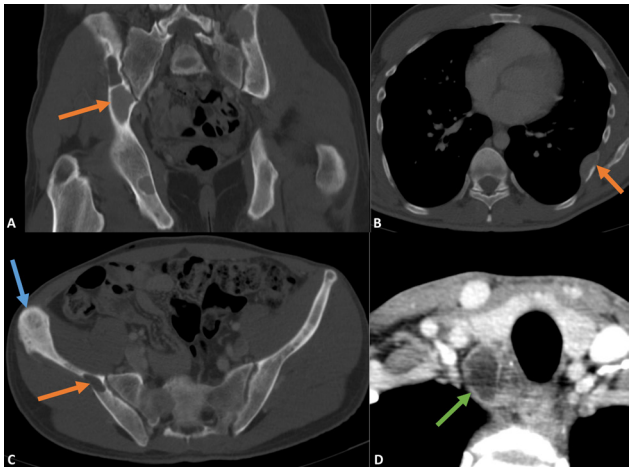


**Figure 10** – Contrast-enhanced CT of the thorax, abdomen, and pelvis. Coronal (A) and axial (B, C) images in bone window demonstrate multiple lytic lesions in the ribs and pelvis (orange arrows) and a sclerotic lesion in the right iliac wing (blue arrow). Axial image in soft-tissue window (D) demonstrates a hypodense cystic mass posterior to the right thyroid lobe (green arrow), suggestive of a parathyroid tumour.

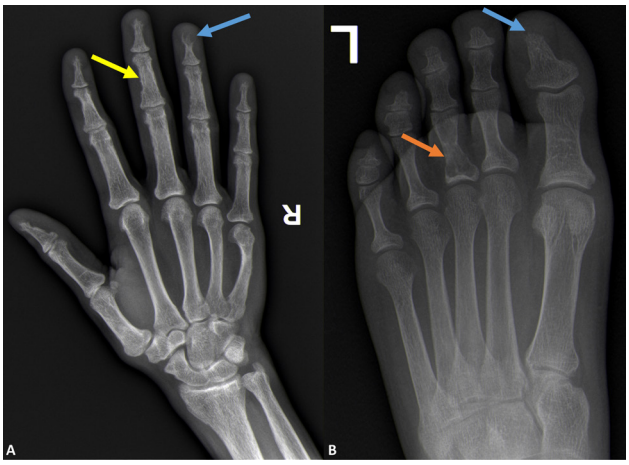


**Figure 11** – Magnified radiographs of the right-hand (A) and left-foot (B) demonstrate acro-osteolysis of the phalangeal tufts of the fingers and toes (examples pointed by blue arrows) and subperiosteal resorption along the radial aspects of the middle phalanges of the fingers (example pointed by yellow arrow), characteristic features of hyperparathyroidism. A lytic lesion in the proximal phalanx of the third toe (orange arrow), consistent with a brown tumour, is also present.

Brown tumours, also known as 'osteitis fibrosa cystica' or 'Von Recklinghausen's disease of the bone', are non-neoplastic focal bone lesions that arise in the setting of prolonged HPT, whether primary, secondary, or tertiary.[18] Excess PTH stimulates osteoclastic bone resorption, leading to replacement of bone by fibrovascular tissue containing multinucleated giant cells. Haemorrhage and subsequent hemosiderin deposition account for the characteristic brown coloration of these lesions.[19] Commonly affected sites include the pelvis, ribs, clavicles, mandible, and long bones, and lesions may be solitary or multiple.[19]

Clinically, brown tumours are often asymptomatic but may present as a palpable, slow-growing bony swelling associated with bone pain or pathological fractures.[20]

On radiographs and CT, brown tumours typically appear as well-defined, expansile lytic lesions with cortical thinning, which may be multiloculated, but they can also be mixed lytic–sclerotic and may even develop a sclerotic rim.[20] They may be solitary or multiple and can be complicated by pathological fracture.[20,21] After correction of the underlying metabolic

abnormality, brown tumours often undergo sclerosis and demonstrate regression.[22]

Additional skeletal manifestations of HPT, including subperiosteal bone resorption, osteopenia, and the "salt-and-pepper" appearance of the skull, may also be observed.[21] Neck ultrasound or CT may demonstrate a parathyroid adenoma in cases of primary HPT.[20] On MRI, brown tumours are usually hypointense to isointense on T1-weighted images and show avid enhancement, although imaging appearances are variable, with three described patterns: solid, cystic, and mixed.[23]

Diagnosis should integrate serum calcium and PTH levels, imaging findings, and the overall clinical context. Biopsy alone is not definitive and may be inconclusive, as brown tumours share histological features with other giant cell–containing lesions.[20,21]

A multidisciplinary approach is essential in determining appropriate management.[21] Treatment is primarily directed at correcting the underlying HPT.[21,24] Orthopaedic management is indicated for impending or actual pathological fractures.[21] Surgical resection of the bone lesions is generally not indicated.[24]

## Gluteus Maximus Calcific Tendinopathy

A 49-year-old woman under follow-up for breast carcinoma presented with low back pain and inability to mobilise her left lower limb. SPECT-CT, performed one month after symptom onset, demonstrated increased uptake in the subtrochanteric region of the right femur, raising suspicion of bone metastasis. She was referred to the Radiology Department for further evaluation and was scheduled two months after symptom onset. By that time, she was asymptomatic, and both the lateral hip radiograph and pelvic CT scan showed no abnormalities (Fig. 12).

Retrospective analysis of the axial CT images in bone windows included in the SPECT-CT revealed an ill-defined, faint calcification at the posterior aspect of the proximal left femur, associated with cortical erosion (Fig. 13), which had been overlooked at the time but was highly suggestive of the final diagnosis.

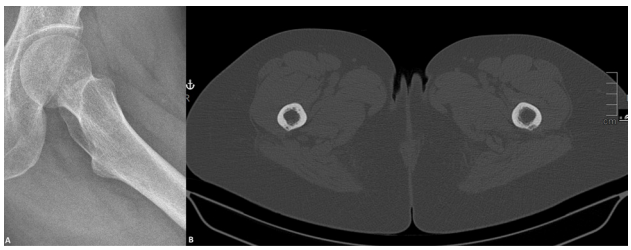

**Figure 12** – Lateral left hip radiograph (A) and axial non-enhanced CT image in bone window (B) are unremarkable. Both were obtained three months after symptom onset.

As the patient had undergone additional imaging at an outside institution, these studies were subsequently obtained. MRI, performed a few days after symptom onset, demonstrated extensive deep soft-tissue oedema adjacent to the posterior femur, surrounding a focal hypointense soft-tissue lesion. A small focus of cortical interruption was present in this region, associated with mild medullary bone marrow oedema (Fig. 14). We also had access to a hip radiograph and CT scan obtained at the same institution one year prior to symptom onset (Fig. 15), which demonstrated a juxta-osseous

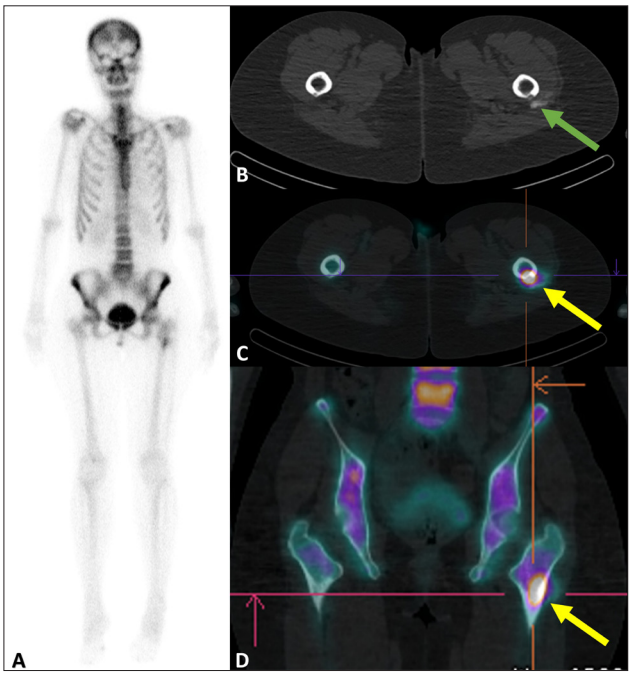


**Figure 13** – Anterior planar image (A), axial low-dose CT (B), and axial (C) and coronal (D) SPECT-CT images, performed one month after symptom onset, demonstrate increased tracer uptake in the left proximal femur (yellow arrows), corresponding to the faint, ill-defined calcification on B (green arrow).

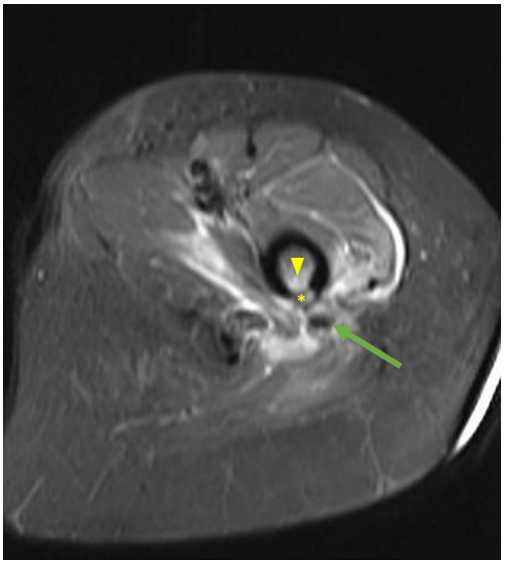

**Figure 14** – Axial T2-weighted MRI image of the left upper thigh, obtained a few days after symptom onset, demonstrates extensive deep soft-tissue oedema adjacent to the posterior femur, a focal hypointense lesion (green arrow), cortical interruption (yellow asterisk), and mild endosteal bone marrow oedema (yellow arrowhead).

calcification at the posterior aspect of the proximal left femur (Fig. 15).

The final diagnosis was calcific tendinopathy of the gluteus maximus with associated bone involvement.

Gluteus maximus tendinopathy is far less common than pathology affecting the gluteus medius and minimus. It encompasses tendinosis, calcific tendinopathy, and partial- or full-thickness tears.[25,26] Calcific tendinopathy of the gluteus maximus results from deposition of calcium hydroxyapatite within the tendon at its femoral insertion at the gluteal tuberosity. It may be asymptomatic but can trigger acute

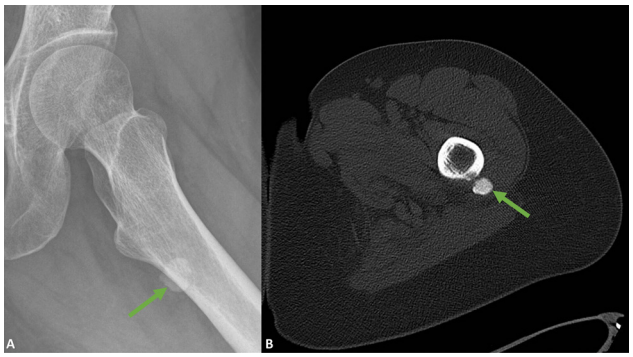

**Figure 15** – Lateral left hip radiograph (A) and axial CT image (B), obtained one year prior to symptom onset, demonstrate a focal, well-defined calcific density along the posterior aspect of the proximal femur (green arrow), corresponding to the gluteus maximus tendon insertion.

inflammatory pain depending on the stage of the disease. This entity is considerably less common in the hip region than in the shoulder.[27]

The condition typically progresses through four stages: precalcific, formative, resorptive, and postcalcific, being usually the resorptive stage the most painful.[27] In our case, we have imaging evidence of the evolution of the calcification through the formative (Fig. 15), resorptive (Figs. 13 and 14), and postcalcific stages (Fig. 12). Patients often present with sudden-onset severe buttock or posterolateral thigh pain, tenderness over the posterior proximal femur, and pain exacerbated by resisted hip extension, sitting, or rising from a seated position.[25,27,28]

Radiographs and CT typically demonstrate peritendinous calcification at the gluteus maximus insertion, sometimes displaying a "comet-tail" morphology.[25,27,28] On MRI, findings are similar to those observed in shoulder calcific tendinopathy. During the resorptive phase, marked soft-tissue oedema may surround the calcific focus. In rare cases, associated cortical erosion and reactive bone marrow oedema may be present.[27,28] These features can mimic osteomyelitis or neoplastic disease and must be interpreted with caution. Calcifications demonstrate low signal intensity and are more readily identified on radiographs than on routine MRI sequences, particularly when small. Therefore, MRI findings should be correlated with radiographs whenever possible.[14] On bone scintigraphy, a peri-insertional focus of increased uptake may be observed, potentially mimicking underlying osseous pathology.[27]

In contrast, bone metastases typically present as intramedullary lesions, which may be lytic, blastic, or mixed depending on the primary tumour, and are not confined to tendon insertions. They are characterised by aggressive marrow replacement, cortical destruction, and tumour matrix or associated soft-tissue mass.[14,29] Moreover, they lack the tendon-centric hydroxyapatite morphology often observed in calcific tendinopathy.

Calcific tendinopathy is usually self-limiting. First-line management includes activity modification, non-steroidal anti-inflammatory drugs (NSAIDs), and physiotherapy. Ultrasound-guided corticosteroid injection or barbotage of the calcification may be performed to reduce symptom duration and severity.[27,28,30]

## Conclusion

Several benign musculoskeletal entities can mimic bone metastases. Recognition of characteristic imaging patterns, such as lateral cortical thickening and a subtrochanteric location in bisphosphonate-related atypical femoral fractures, marrow fat sparing, linear fracture lines, and posterior bony retropulsion in osteoporotic vertebral compression fractures, well-defined expansile lytic lesions associated with ancillary signs of hyperparathyroidism in brown tumours, and intratendinous or periarticular calcifications in calcific tendinopathy, can prevent delayed or misdiagnosis and inappropriate treatment.

When diagnostic uncertainty persists, multidisciplinary discussion involving a radiologist is essential, together with careful clinical and laboratory correlation, short-interval imaging follow-up, and biopsy when indicated.

**Ethical Disclosure / Divulgações Éticas**

*Conflicts of interest*: The authors have no conflicts of interest to declare.

*Conflitos de interesse*: Os autores declaram não possuir conflitos de interesse.

*Financing Support*: This work has not received any contribution, grant or scholarship.

*Suporte financeiro*: O presente trabalho não foi suportado por nenhum subsídio ou bolsa.

*Confidentiality of data*: The authors declare that they have followed the protocols of their work center on the publication of data from patients.

*Confidencialidade dos dados*: Os autores declaram ter seguido os protocolos do seu centro de trabalho acerca da publicação dos dados de doentes.

*Protection of human and animal subjects*: The authors declare that the procedures followed were in accordance with the regulations of the relevant clinical research ethics committee and with those of the Code of Ethics of the World Medical Association (Declaration of Helsinki).

*Protecção de pessoas e animais*: Os autores declaram que os procedimentos seguidos estavam de acordo com os regulamentos estabelecidos pelos responsáveis da Comissão de Investigação Clínica e Ética e de acordo com a Declaração de Helsínquia da Associação Médica Mundial.

**References**

1. Shane E, Burr D, Ebeling PR, Abrahamsen B, Adler RA, Brown TD, et al. Atypical subtrochanteric and diaphyseal femoral fractures: report of a task force of the American society for bone and mineral research. Journal of Bone and Mineral Research. 2010 Oct 25;25:2267-94.

2. Lloyd AA, Gludovatz B, Riedel C, Luengo EA, Saiyed R, Marty E, et al. Atypical fracture with long-term bisphosphonate therapy is associated with altered cortical composition and reduced fracture resistance. Proceedings of the National Academy of Sciences of the United States of America. 2017 Aug 15;114:8722-7.

3. Aapro M, Saad F, Costa L. Optimizing clinical benefits of bisphosphonates in cancer patients with bone metastases. The Oncologist. 2010 Nov;15:1147-58.

4. Dionísio MR, Mansinho A, Abreu C, Cavaco-Silva J, Casimiro S, Costa L. Clinical and translational pharmacology of drugs for the prevention and treatment of bone metastases and cancer-induced bone loss. British Journal of Clinical Pharmacology. 2019 Feb 16;85:1114-24.

5. Drake MT, Clarke BL, Khosla S. Bisphosphonates: mechanism of action and role in clinical practice. Mayo Clinic Proceedings. 2008 Sep;83:1032-45.

6. Tile L, Cheung AM. Atypical femur fractures: current understanding and approach to management. Therapeutic Advances in Musculoskeletal Disease. 2020;12:1759720X20916983.

7. Yli-Kyyny T. Bisphosphonates and atypical fractures of femur. Journal of Osteoporosis. 2011;2011:1-5.

8. Edwards BJ, Bunta AD, Lane J, Odvina C, Rao DS, Raisch DW, et al. Bisphosphonates and nonhealing femoral fractures: analysis of the FDA Adverse Event Reporting System (FAERS) and international safety efforts: a systematic review from the Research on Adverse Drug Events And Reports (RADAR) project. J Bone Joint Surg Am. 2013;95:297-307.

9. Khan AA, Kaiser S. Atypical femoral fracture. Canadian Medical Association Journal. 2017 Apr 9;189:E542-2.

10. Bhadada SK, Sridhar S, Muthukrishnan J, Mithal A, Sharma DC, Bhansali A, et al. Predictors of atypical femoral fractures during long term bisphosphonate therapy: a case series & review of literature. Indian Journal of Medical Research. 2014;140:46-54.

11. Jain T, Thorn M. Atypical femoral fractures related to bisphosphonate therapy. Indian Journal of Radiology and Imaging. 2012;22:178.

12. Larsen MS, Schmal H. The enigma of atypical femoral fractures. EFORT Open Reviews. 2018 Sep;3:494-500.
13. Larsen MS, Schmal H. The enigma of atypical femoral fractures. EFORT Open Reviews. 2018 Sep;3:494–500.
14. Major NM, Anderson MW. Musculoskeletal MRI. Elsevier; 2019.
15. Mauch JT, Carr CM, Cloft H, Diehn FE. Review of the imaging features of benign osteoporotic and malignant vertebral compression fractures. American Journal of Neuroradiology. 2018 Jan 18;39:1584-92.
16. Jung H-S, Jee W-H, McCauley TR, Ha K-Y, Choi K-H. Discrimination of metastatic from acute osteoporotic compression spinal fractures with MR imaging. Radiographics. 2003;23:179-87.
17. Baker LL, Goodman SB, Perkash I, Lane B, Enzmann DR. Benign versus pathologic compression fractures of vertebral bodies: assessment with conventional spin-echo, chemical-shift, and STIR MR imaging. Radiology. 1990 Feb;174:495—502.
18. Vaishya R, Agarwal AK, Singh H, Vijay V. Multiple "Brown Tumors" masquerading as metastatic bone disease. Cureus. 2015 Dec 23;7:e431.
19. Carsote M, Ciobica ML, Sima OC, Valea A, Bondor CI, Geleriu A, et al. Brown tumors: the hidden face of primary and renal hyperparathyroidism amid real-life settings. Journal of Clinical Medicine. 2024 Jun 29;13:3847.
20. Xie C, Tsakok M, Taylor N, Partington K. Imaging of brown tumours: a pictorial review. Insights into Imaging. 2019 Jul 29;10:75.
21. Karaca MO, Özyıldıran M, Savran MD, Başarır K, Yıldız HY. Brown tumors: retrospective analysis of 26 cases. Archives of Orthopaedic and Trauma Surgery. 2024;144:2927-34.
22. Rautray P, Tomar K, Roy ID, Singh AK. Management modalities of aggressive brown tumor of the jaws-a case series. Journal of Oral and Maxillofacial Surgery. 2024;23:688-91.
23. Herrera Ortiz AF, Olarte L, del Castillo V, Duarte JN, Rojas J, Aguirre D. Brown tumors mimicking multiple myeloma: a case report. Radiology Case Reports. 2025 Jan;20:841-5.
24. Can Ö, Boynueğri B, Gökçe AM, Özdemir E, Ferhatoğlu F, Canbakan M, et al. Brown tumors: a case report and review of the literature. Case Reports in Nephrology and Dialysis. 2016 Mar 18;6:46-52.
25. Tran S, North T, Hackel JG. Calcific tendinitis of gluteus maximus insertion. Radiology Case Reports. 2024 Sep;19:3748-51.
26. Samra A, Loh AK, Littlewood A, Oyibo SO. Bilateral gluteus maximus tendon tear following an apparently low-impact trauma: a case report. Cureus. 2025;17:e81490.
27. Damme KV, Coster LD, Koen Mermuys, Van A, Geeter FD. Bone scan findings in calcific tendinitis at the gluteus maximus insertion: some illustrative cases. Radiology Case Reports. 2017 Jan 17;12:168-174.
28. Huang K, Murphy D, Dehghan N. Calcific tendinitis of the gluteus maximus of a 53-year-old woman. Canadian Medical Association Journal. 2017;189:E1561.
29. Helms CA. Fundamentals of skeletal radiology. Elsevier. 2019.
30. Arirachakaran A, Boonard M, Yamaphai S, Prommahachai A, Kesprayura S, Kongtharvonskul J. Extracorporeal shock wave therapy, ultrasound-guided percutaneous lavage, corticosteroid injection and combined treatment for the treatment of rotator cuff calcific tendinopathy: a network meta-analysis of RCTs. European Journal of Orthopaedic Surgery & Traumatology. 2016 Aug 23;27:381-90.